An X-ray Mapper for the Mu2e Experiment

S. H. Oh, C. Wang
Department of Physics
Duke University
Durham, NC, USA, 27708

Abstract

We report on the construction and performance of a scanner using a collimated x-ray beam to find the positions of wires, straws, slots and spheres. The technique is based on measuring the transmission rate of the beam, and their positions can be determined ~ 25 μm accuracy. The spheres or slots attached to the detector can also be optically surveyed externally to transfer the coordinates of wires and straws to other detector systems. The scanner was developed for the Mu2e straw tracker but may have a wide range of applications.

1. Introduction

It has been nearly 50 years since detectors based on the multi-wire technique were developed [1]. Multi-wire detectors are still widely utilized in many experiments to measure the trajectory of charged particles, and one of the latest applications is the Mu2e straw tracker [2] based on 5 mm diameter straw tubes. The Mu2e experiment at the Fermi National Accelerator Laboratory will search for charged lepton flavor violation with unprecedented sensitivity. The experiment will measure the ratio of the coherent neutrinoless conversion in the field of a nucleus of a negatively charged muon into an electron to the muon capture process [2].

The position resolution of particles measured by the detector depends on several factors. One is the intrinsic detector resolution, and another is the position uncertainty of anode wires, where ionized electrons are collected. Since the typical intrinsic resolution of drift wire detectors is around 150 μm, the wire location should be known much better than the resolution. The wire position requirements of the Mu2e tracker are 75 μm perpendicular to the magnetic field and 1 mm along the direction of the magnetic field. In this paper, we report on the construction and testing of a scanner developed for the Mu2e experiment to determine the wire and straw positions in three dimensions.

In a previous paper, a wire scanner constructed for the ATLAS Transition Radiation Tracker (TRT) and its various applications were reported [3]. The TRT scanner also utilizes a collimated x-ray beam, but the technique depends on detecting electrons produced when x-ray photons interact with material. Because it has to detect the knocked out electrons, the detector being scanned has to be in operation, which requires front-end electronics and ADCs for all wires, resulting in a somewhat cumbersome procedure.

The new technique does not require operating the detector since it depends on measuring the transmission rate as the x-ray beam traverses the material. Unlike the previous scanner, the material can be not only wire and straw, but also any other shape such as a sphere or slot.

2. Design and Construction of the Scanner

There are two main components of the scanner. One is the x-ray tube, and the other is a linear slide with a stepper motor. The x-ray tube was made by Oxford Instruments (model 93000) [4]. The anode HV ranges from 10 to 50 kV, and the maximum current is 1 mA. The average beam size at the anode is about 100 μm measured by the manufacturer. The slide (model EZS6E085-A) and controller (model SCX11) were made by Oriental Motor [5]. The travel distance of the slides used in the scanner is 85 cm, and the accuracy specification for the slide and stepper motor combination is 10 μm, including the repeatability.

Operated by Fermi Research Alliance, LLC under Contract No. De-AC02-07CH11359 with the United States Department of Energy.

The accuracy was checked by moving the slide back and forth many times and measuring the slide's positions using dial gauges fixed on the optical table where the scanner is located. Figure 1 shows a schematic of the scanner, and Figure 2 shows a picture of the x-ray assembly.

There are two slides covering the xy-plane[1]. The first slide, which moves along the x-axis, is mounted on an U-channel, and the second slide, which moves along the y-axis, is mounted on the first one. The x-ray tube is attached to the y-slide. A 20 cm long brass tube with 6.25 cm outer diameter and 3 mm thickness is attached to the x-ray window to contain the beam. The end of the tube is covered with a slit also made of brass. The width and the length of the slit can be adjusted, and the slit can rotate slightly with respect to the tube to adjust the beam direction. The maximum slit width is 2 mm, and the maximum slit length is 5 cm. The slit or the beam direction (the long side) is along the x-axis, the same as the wire direction as shown in Figure 3. Below the slit, a detector or material to be scanned and an x-ray detector are positioned. There are two types of scans, x-scan and y-scan. The x-scan (y-scan) is when the beam moves along the x-axis (y-axis).

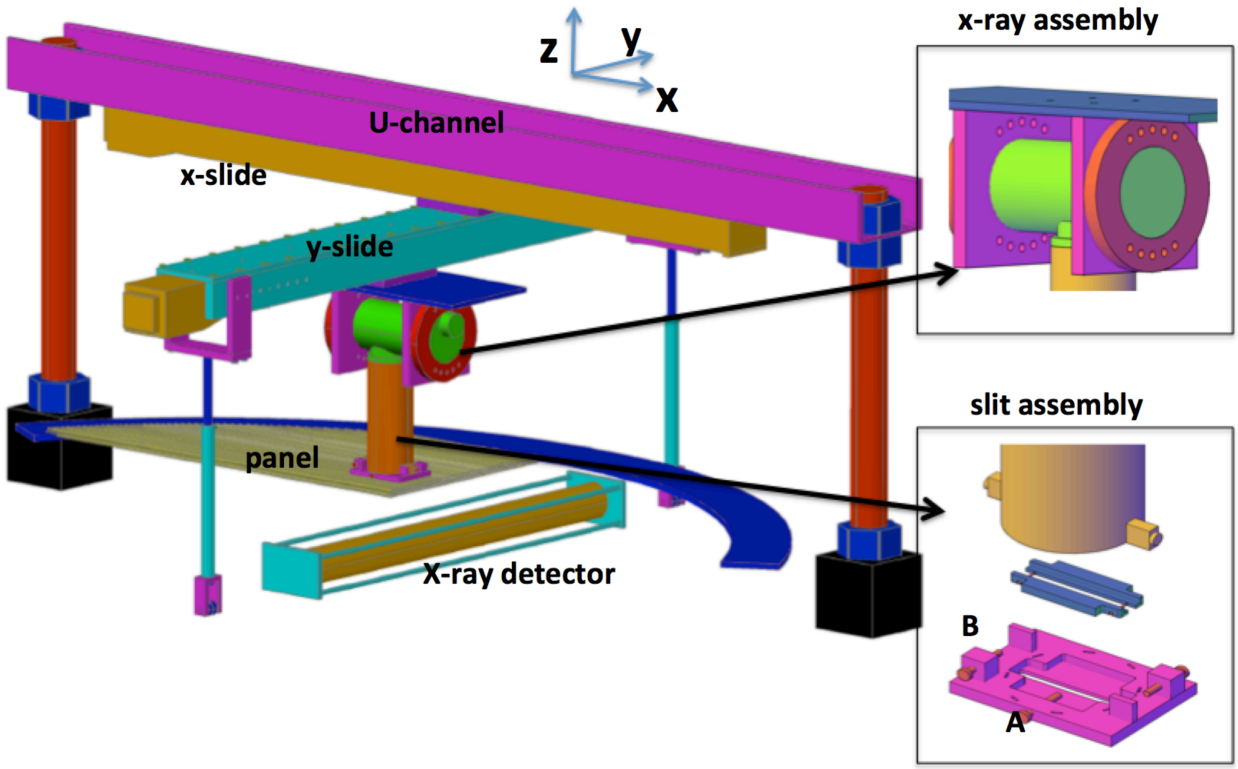

Figure 1. Mu2e x-ray scanner. The x-slide is attached to a 130 cm long U-channel supported by two large vertical screws on an optical table. The y-slide is attached to the x-slide, and the x-ray tube and slit assembly are attached to the y-slide. Below the slit, a Mu2e straw detector panel and the x-ray detector are shown. Top insert: The x-ray tube is fixed to the ring (red color), which can be rotated with respect to the support (purple color) around the x-axis for a stereo measurement. The holes are for dowel pins to fix the angle. Bottom insert: The slit assembly. The slit width can be adjusted using screw A and rotated a few degrees with respect to the tube using screw B for an alignment purpose. See Figure 2 for a picture of the x-ray tube and slit assembly.

[1] Our coordinate system is such that the wire plane is on the xy-plane (horizontal), and wires are along the x-axis. The z-axis is along the vertical direction. It is worthwhile to mention that, in the real experiment, the wire planes are perpendicular to the magnetic field lines.

The panel shown in Figure 1 and consisting of 96 straws is the basic unit of the Mu2e straw detector. Twelve panels form a ring-shaped station, and there are 216 panels corresponding to 18 stations. The straw tubes are perpendicular to the magnetic field direction, and the length of the shortest straw is 47.5 cm, and the longest straw is 120.6 cm.

The detection of the x-rays was done with a straw tube detector. The tube with 5 cm inner diameter was made of aluminized paper and Mylar film, and the thickness of aluminum, paper, and Mylar are 12, 100, and 75 μm respectively. The anode wire was 30 μm diameter gold plated tungsten wire under a tension of 0.7 N. A mixture of Ar (80 %) and CO_2 (20 %) was used for the ionization gas. The efficiency of detecting a photon depends on the photon energy and path length inside the straw tube. For example, for 10, 15, and 20 keV photons, the maximum efficiency calculated using XCOM [8] is about 45, 15, and 5 % respectively. The interaction cross section at these energies is dominated by the photoelectric absorption. The efficiency can be easily increased by replacing Ar with Xe or Kr. However, high efficiency is not important because our technique depends on measuring the change in the transmission rate due to material. The large radius straw tube detector is a good choice since it covers a large area cheaply.

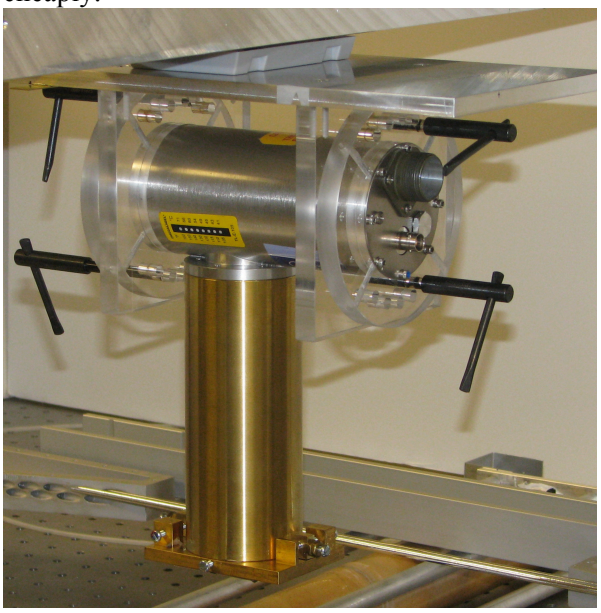

Figure 2. A picture of the x-ray tube and slit assembly. The assembly can be rotated in steps of 15 degrees around the x-axis for a stereo measurement. Four pins to fix the angle are shown.

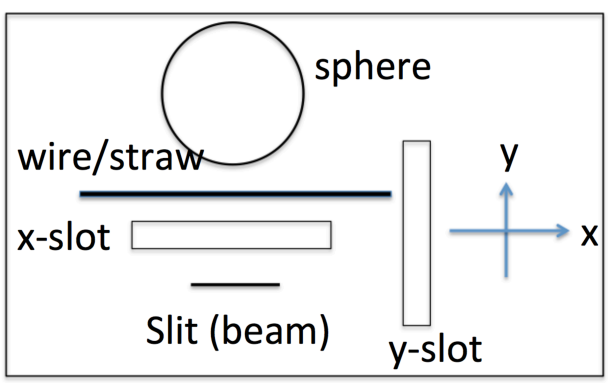

Figure 3. The shapes used to test the scanner. Shapes are not to scale. The wire, straw and x-slot are measured with a y-scan. The y-slot is measured with an x-scan. The sphere is measured with both an x-scan and y-scan. The slit (beam) can be rotated by a couple of degrees around the z-axis for alignment purposes.

3. Wire Position Measurement

We placed three pieces of wire with different diameters (25, 75 and 100 μm) under tension. They were 5 cm below the slit, and the straw tube x-ray detector was positioned below the wires. The first step to measure the wire position was to align the slit (beam) along the wire direction using screw B in Figure 1. This was accomplished by minimizing the width of the absorption curve in a beam transmission plot shown in Figure 4. Plotted is the x-ray counting rate as a function of the slit's y position (y-scan). For the plot, the x-ray tube was moved with 20 μm steps, and the x-ray counting rate (transmission) was recorded using USB-1608FS DAQ device made by MCC [6]. The DAQ device and the stepper motors were controlled with LabVIEW software. The exact alignment is not critical since the wire position corresponds to the center of the valley. We point out that the default settings for the HV and current of the x-ray tube were 10 kV and 0.01 mA respectively. The default dimensions for the slit were 30 μm in width and 4.5 mm in length. With the default values, the counting rate was about 2500 Hz.

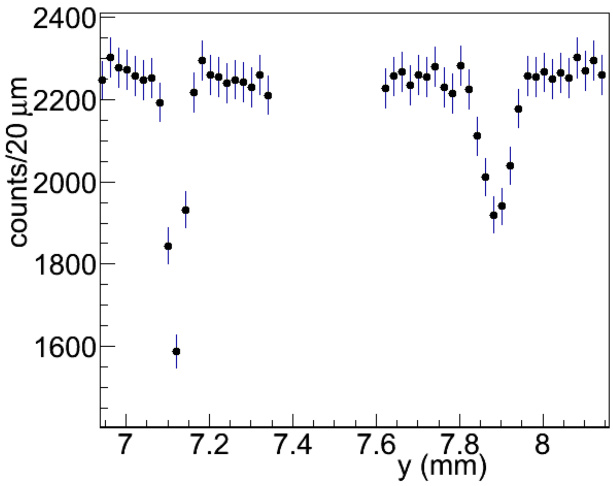

Figure 4. The counting rate as a function of y as the beam moves across 25 μm diameter wire. The plot shows the effect of misalignment between the beam and wire. The first valley corresponds to the case in which the beam and wire are well aligned. The second valley is the case in which the two are misaligned by one degree.

Figure 5 shows a result of a y-scan of the three wires that are clearly visible. The valleys are fitted with a Gaussian function and the results are listed in Table 1. From the table, we can conclude that the wire position can be located with accuracy better than a few microns. However, the actual accuracy is dictated by the linear slide's accuracy, which is 10 μm. The sigma in the table reflects the wire diameter plus beam width, as well as the beam to wire alignment. The three-wire setup was scanned several times for a reproducibility study and the wire positions from all scans were consistent with each other.
The measurement was also cross-checked by measuring the distance between wires using a traveling microscope and found to be consistent with the scan results.

With the x-ray beam perpendicular to the xy-plane, only the y displacement of wires can be measured. However by rotating the beam by an angle around the x-axis (stereo method), the z position can be measured as well (Figure 6), thus completely determining the wire position in three dimensions. In our design, the x-ray tube can rotate from - 30 degrees to 30 degrees with a 15 degree step (see Figure 1 and 2). It is worthwhile to note that measuring the rotation angle accurately is not necessary. For the 15 degree rotation, if the uncertainty of the angle is 1 degree, the uncertainty in the z position would increase by ~1/15 or ~ 7 %.

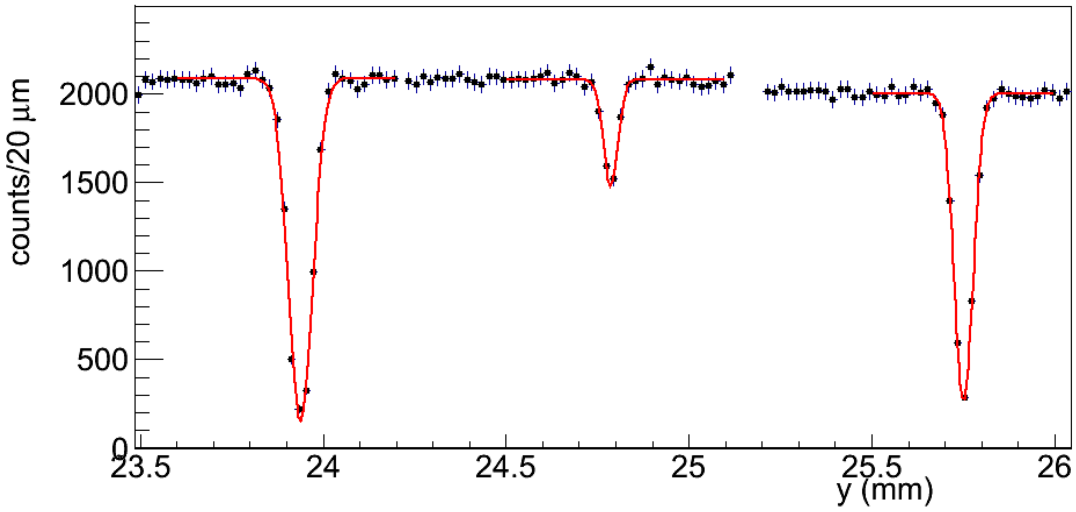

Figure 5. The counting rate from a scan of the three wires. From the left, the three valleys correspond to 100, 25 and 75 µm diameter wire respectively. The curves are from fits.

diameter	position uncertainty	Sigma
25 µm	1.6 µm	20 µm
75	0.6	31
100	0.5	35

Table 1. The results (second and third column) from fitting the valleys with a Gaussian function in Figure 5.

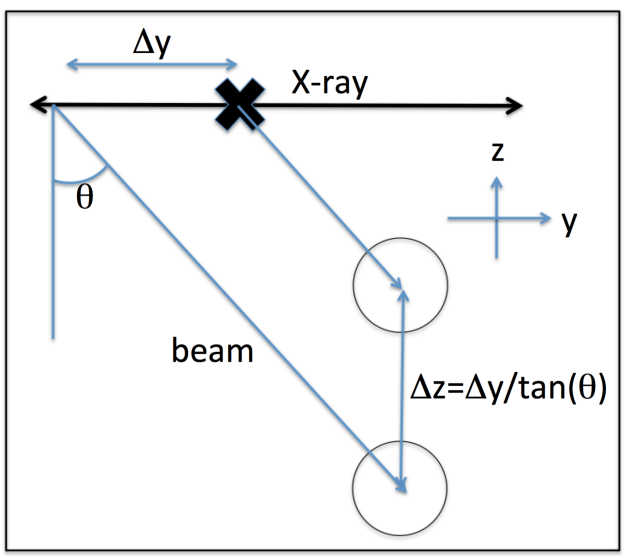

Figure 6. A schematic for the stereo method. One straw is displaced by Δz. By rotating the beam around the x-axis by θ, Δz is calculated from Δy.

One problem with the scanner is that the slides do not move on a perfectly flat plane. The x-ray beam has a slight slope with respect to the z-axis as a function of x and y because of the mechanical limitation of slides and our machining tolerance. The slope causes a shift from the true x and y position by Ldx/dz and L'dy/dz respectively where L and L' are the distances from the wire to the slides and dx/dz and dy/dz are the x and y slopes of the beam. In order to preserve better than 25 µm accuracy, the slopes should be less than 0.005 degree, which was difficult to achieve mechanically. Thus we measured the beam slopes and corrected the wire position.

There were several digital levels meeting the accuracy requirement, and our choice was DWL-5500XY made by Digi-Pas [7]. This measures x and y slopes simultaneously and has 0.001 degree accuracy. The two slopes were read out every time the beam was moved with the LabVIEW program. The maximum correction for our scanner is about 100 μm, and the uncertainty of this correction, about 5 μm, is another factor limiting the scanner's accuracy.

Other limitations are that the slides do not move along a straight line and the angle between slides is not exactly 90 degrees. The first effect can be easily calibrated out by measuring a long wire under tension, and our slides moves straight well within +/- 20 microns. This calibration contributes another ~ 10 micron uncertainty. The angle between slides was measured using a precision square[2]. As discussed in section 5, straight edges can be easily measured with high precision. This introduces less than 10 micron uncertainty.

4. Straw Diameter Measurement

The Mu2e straw was made of Mylar film and the outer diameter is 5.03 +/-0.03 mm. The wall thickness is 15 μm of which 2/3 is due to the Mylar film, and the glue between two layers of Mylar film contributes the rest [2]. Figure 7 shows a result of a y-scan, and the two ends of the straw are visible. The axis of the straw is along the x-axis. From the plot, we obtain 5.06 +/- 0.04 mm for the straw outer diameter, which is consistent with the expected diameter, but the comparison is difficult because the straw tube may not be perfectly round[3]. The straw position is useful since the operational stability requires keeping the minimum distance between the anode wire and the straw wall. The distance is easily obtainable by finding the locations of the straw center and the anode wire in three dimensions using the stereo method.

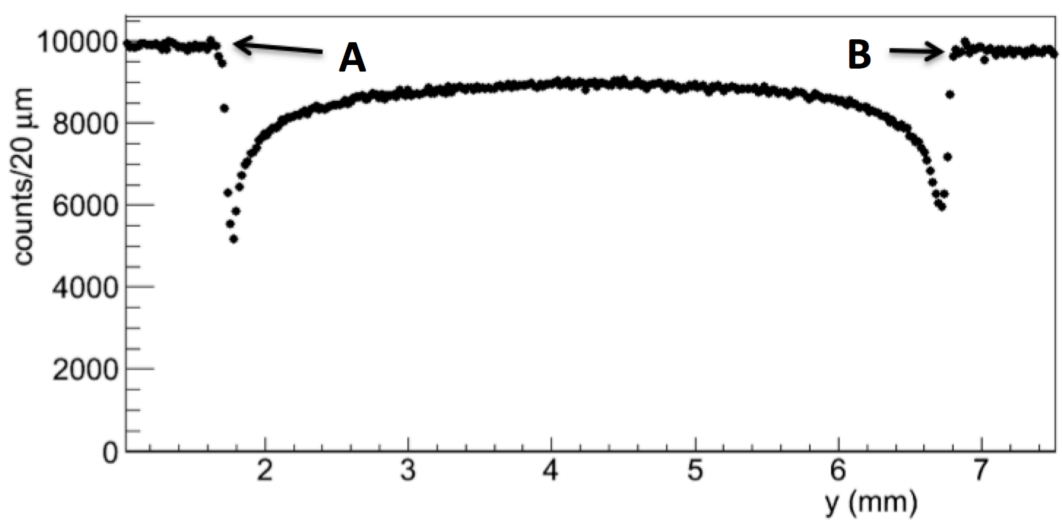

Figure 7. A y-scan of a Mu2e straw. The shape reflects the straw wall material projected on the xy-plane. The distance between two valleys is 4.92 +/- 0.03 mm. The distance between A and B is 5.09 +/- 0.03 mm, which equals the straw outer diameter plus the beam width. The position of A or B corresponds to the data point where the counting rate starts to decrease, and an uncertainty of +/- 0.02 mm is assigned to the position.

[2] Another way to measure the angle accurately between two slides is to flip the square, re-measure the angle and compare the two. This method does not require a precision square.

[3] The straw diameter was only approximately calculated (see Figure 7 caption) because the true straw diameter was difficult to obtain for a comparison. In the next section, we employ a different analysis method for slots and spheres for more accurate results. The same technique can be applied here.

5. Slot and Sphere Measurement

It is necessary for the wire positions to be tied to a reference point on the detector that can be scanned with the wires, as well as optically measured externally. This requirement will provide the absolute wire coordinates with respect to other detector systems. This goal can also be accomplished using straight tracks through the detector, but for the Mu2e experiment, using tracks may not be feasible. The reference point could be a precision ball or slot. Mu2e will utilize survey balls and possibly slots attached to panels. In this section, we demonstrate that the position of a ball and slot can also be accurately measured.

Eight slots were machined in a 1.6 mm thick brass plate in two directions and measured. Four slots were x-slots along the y-axis and the other four were y-slots along the x-axis (see Figure 3). The slot width is 1.00 +/- 0.03 mm, and the distance between slots is 150.00 +/- 0.03 mm. The uncertainties are from the machining tolerances. Figure 8 shows typical transmission data for a y-scan of an x-slot. The rising edge and falling edge data are fitted using a hyperbolic tangent function separately. From the fit, the slot width and the distance between slot centers are calculated and we obtain 0.984+/- 0.020 mm and 150.05 +/- 0.04 mm respectively. A good way to calculate the slot center (or width) is to find the midpoint of the rising and falling edges from fits and calculate the average (or difference) of the two midpoints. The uncertainties include statistical uncertainties as well as the systematic uncertainties due to the slide accuracy, slope correction and the fitting procedure.

Figure 9 shows transmission data for an x-scan of a y-slot. The data are divided into five regions as shown in the figure. Each region is fitted with a linear function and the four intersections between linear functions are calculated. From the intersections, the slot width and the distance between slot centers are calculated and we obtain 0.98+/-0.03 mm and 150.02+/-0.03 mm respectively, which are quite consistent with the expected values. The slot measurements demonstrate scale accuracy consistent with the scanner resolution over 450 mm travel in x and y.

A stainless steel ball with 12.700 +/- 0.001 mm diameter was scanned. Figure 10 shows a y-scan and Figure 11 shows an x-scan. Unlike the y-scan of a slot (Figure 8), the rising and falling edges in Figure 10 are not sharp because of the circular boundary. The radius from each scan is calculated by fitting the rising and falling edges and the plateau regions as described in Figure 9. The calculated diameters are 12.68 +/- 0.04 mm from the y-scan and 12.65 +/- 0.03 mm from the x-scan. Despite the circular boundary of the ball, the results are good. The center of the sphere can be easily found as previously discussed. Although not demonstrated, we should be able to measure holes with similar precision.

6. Conclusion

We reported on the construction and performance of an x-ray scanner developed to scan panels of the Mu2e straw tracker and based on the x-ray transmission rate as the x-ray beam moved over different material. We demonstrated that the accuracy in locating wires, straws, spheres, and slots was ~ 25 μm and limited by the slide's intrinsic accuracy and the x-ray beam slope-correction uncertainty. Using the stereo method, three-dimensional mapping of wires and straws can be established. The markers such as spheres and slots can be scanned together with wires and also optically measured, thus providing a way to transform the wire locations to the coordinate system of other detectors.

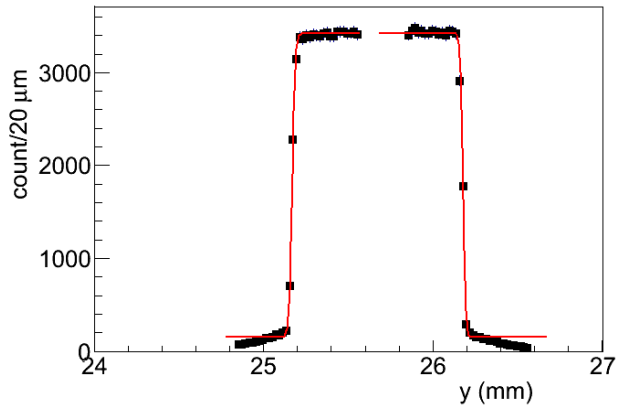

Figure 8. A y-scan of an x-slot. The step size is 20 µm. Note the sharp rise and fall at the slot boundaries. The gap in the middle is because the data were not taken to reduce the scanning time. The curves are from fits described in the text. The center of the slot and the slot width are obtained from the midpoint of the rising and falling edges calculated from fits.

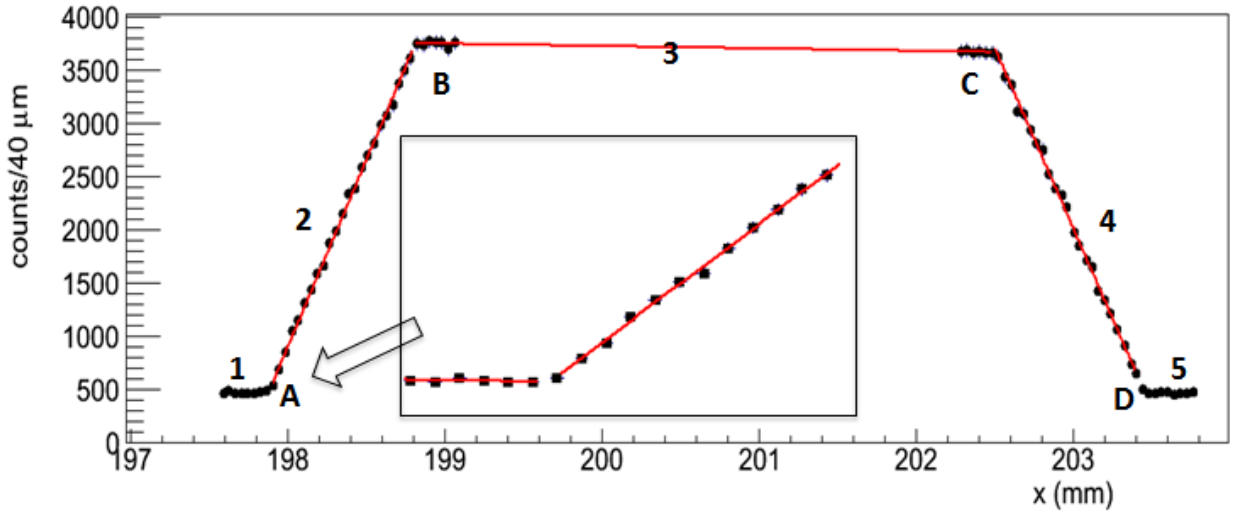

Figure 9. An x-scan of a y-slot. The step size is 40 µm. The lines are from fits. The gap in the middle is because the data were not taken to reduce the scanning time. Intersection A is when the right edge of the beam enters the slot (beam is moving along the positive x-axis, see Figure 3), B is when the right beam edge leaves the slot, C is when the left beam edge enters the slot, and D is when the beam leaves the slot entirely. The distance between A and B or C and D is the slot width. The distance between B and C is the beam length minus the slot width.

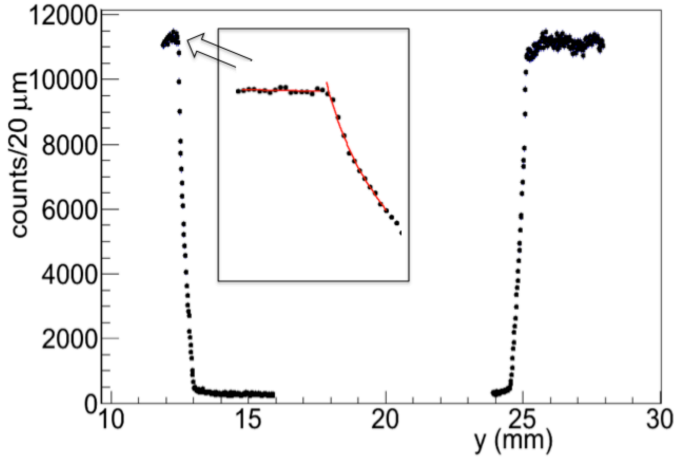

Figure 10. A y-scan of a stainless steel ball. Unlike Figure 8 (y-scan of a slot), the rising and falling edges are not sharp. This is because the boundary with respect to the beam is circular (Figure 3). The lines are from fits to find the intersection point. The distance between the upper left intersection and upper right intersection corresponds to the ball diameter plus the beam width.

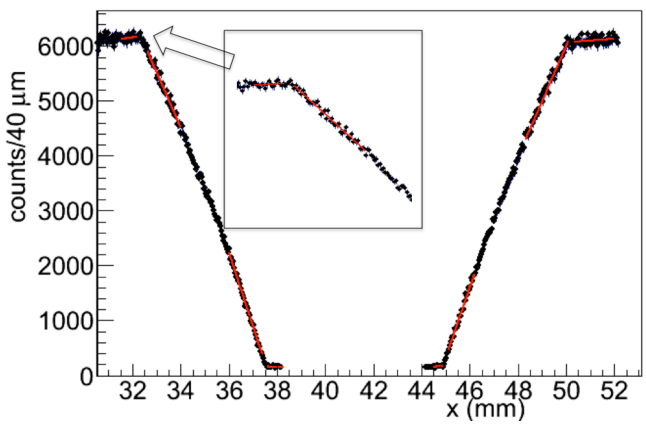

Figure 11. An x-scan of a stainless steel ball. The lines are from fits. The ball diameter is the distance between the upper left (right) intersection and the lower right (left) intersection. The shape of the plot is quite different from the y-scan (Figure 10) because of the shape of the beam (Figure 3).

Acknowledgement

We thank our funding agency, the U.S. Department of Energy (DoE DE-SC0010007-2), for supporting personnel and the Duke University Physics Machine Shop for producing components. The authors are also grateful to the Mu2e collaboration for its support (DoE DE-AC02-05CH11231 and DE-AC02-07CH11359).

References

[1] G. Charpak et al., Nuclear Instruments and Methods 62 (1968) 235
[2] L. Bartoszek, et al.,Mu2e Technical Design Report, arXiv:1501.05241
[3] T. Akesson et al., Nuclear Instruments and Methods A 507 (2003) 622
[4] http://www.oxford-instruments.com/products/x-ray-tubes-and-integrated-sources/x-ray-tubes,
[5] http://www.orientalmotor.com/
[6] http://www.mccdaq.com/
[7] http://www.digipas.com/
[8] http://physics.nist.gov/PhysRefData/Xcom/html/xcom1.html